Available online at www.sciencedirect.com
SCIENCE DIRECT®
ELSEVIER
Journal of Contaminant Hydrology 62–63 (2003) 303–318
JOURNAL OF Contaminant Hydrology
www.elsevier.com/locate/jconhyd

Modeling unsaturated flow and transport processes at the Busted Butte Field Test Site, Nevada

P.-H. Tseng[a,*], W.E. Soll[b], C.W. Gable[a], H.J. Turin[c], G.Y. Bussod[a,1]

[a] *Hydrology, Geochemistry, and Geology Group, EES-6, MS-T003, Los Alamos National Laboratory, Los Alamos, NM 87544, USA*
[b] *Environmental Dynamics and Spatial Analysis Group, EES-10, MS-J495, Los Alamos National Laboratory, Los Alamos, NM 87544, USA*
[c] *Isotope and Nuclear Chemistry Group, C-INC, MS-J534, Los Alamos National Laboratory, Los Alamos, NM 87544, USA*

Abstract

A numerical model was used to simulate the flow and transport processes at the Busted Butte Field Test Site for the purpose of quantifying the effects of hydrogeologic conditions beneath the potential Yucca Mountain repository horizon. In situ experiments were conducted on a $10 \times 10 \times 7$ m block comprising a layered Topopah Springs/Calico Hills formation with two imbedded faults. Tracer solution was continuously injected in eight parallel boreholes arranged on two horizontal planes. Twelve collection boreholes were emplaced perpendicular to the injection holes and were both horizontal and inclined. Solution samples were collected regularly using a sampling assembly consisting of an inverted membrane and sorbing-paper sampling pads. Comparisons between measurements and predictions show that, except for the occasional drops of concentrations observed in the field, the current model is able to capture the general characteristics of the system with varying levels of agreement using laboratory-measured mean hydraulic properties. Simulation results and field observations revealed a capillary-driven flow in the system. Good quantitative agreement is generally observed for near-field boreholes, however, this agreement deteriorates and the simulated solute concentration is underestimated at boreholes farther away from the injection points. Increasing the spatial resolution of the simulation improves the model predictions only to a limited extent. Scaling issues may need to be considered to describe flow and transport events, as the travel distance becomes large.

Keywords: Unsaturated flow and transport; Numerical modeling; Field tracer test; Flow and transport in tuffs

* Corresponding author. Tel.: +1-505-667-5518; fax: +1-505-665-8244.
E-mail address: tseng@lanl.gov (P.-H. Tseng).
[1] Currently at Science Network International, Inc., Santa Fe, New Mexico.

0169-7722/02/$ - see front matter © 2002 Elsevier Science B.V. All rights reserved.
doi:10.1016/S0169-7722(02)00163-8

1. Introduction

For approximately 20 years, the US Department of Energy has directed a large research program aimed at evaluating the performance of a potential, high-level radioactive waste (HLW) repository at Yucca Mountain, Nevada. A major challenge of this program is the highly coupled nature of thermal, hydrological, chemical, and mechanical processes involved in a complex geologic setting. Additionally, we must make reliable prediction of the system performance over tens of thousands of years into the future. Hence, process-based models become indispensable tools for the integration of available knowledge and for the extrapolation of information gained from a limited number of field studies.

While models have provided, and will continue to provide, a descriptive framework for research and management needs, they are also subject to a large number of simplifying assumptions that limit their applicability to many practical problems in the field. Foremost among these is the limitation imposed by data acquisition due to the overwhelming heterogeneity occurring at a hierarchy of spatial and temporal scales in the subsurface environment. Parameters measured at one scale will typically fail to describe the processes operative at a different scale. To build confidence on long-term predictions, model validation is an important issue for the performance assessment of HLW repository (Eisenberg et al., 1999).

The Busted Butte unsaturated zone transport test (UZTT) was conducted for this purpose due to the presence of a readily accessible exposure of major stratigraphic units beneath the potential Yucca Mountain repository horizon (Bussod et al., 1999). An integrated field, laboratory, and modeling effort has been designed to quantify the effects of hydrogeologic conditions believed to be operative at the Yucca Mountain repository site. One major goal of the Busted Butte UZTT is to help evaluate the fundamental processes and the degrees of uncertainties associated with flow and transport in the Yucca Mountain unsaturated zone site-scale models. Modeling of flow and transport at Busted Butte has been used to identify additional data needs for a more refined modeling exercise and to assist in the development of activities for a better understanding of the system.

This paper presents an initial effort in modeling flow and transport processes at the Busted Butte UZTT. A conceptual model was developed to approximate the physical system using available data. The reliability of model predictions was evaluated by comparing the simulation results with the field observations. The deficiencies in using the current model to describe water flow and solute transport observed at the field were identified and summarized. Finally, the possible topics for future work using available approaches to gain better understanding of the physical system are discussed.

2. Busted Butte unsaturated zone transport test

The Busted Butte unsaturated zone transport test (UZTT) started in the summer of 1998 as part of the Yucca Mountain site characterization effort. Tracer injection was terminated on October 30, 2000. This section briefly describes the experimental setup at Busted Butte. A more detailed description concerning the scope, configuration, and test design can be found in Bussod et al. (1999).

2.1. Site description and experimental design

Busted Butte is a small, north-trending mountain block located approximately 8 km southeast of the potential Yucca Mountain repository area. The site was chosen because of the presence of a readily accessible exposure of the Topopah Springs/Calico Hills formations and its similarity to the formations beneath the potential Yucca Mountain repository horizon. As such, it is a valuable site for studying flow and transport processes that are crucial for performance assessment of the repository system.

The underground test facility is located on the southeast side of Busted Butte within a main adit and a test alcove approximately 70 m below ground surface. Injection and sampling of tracers were carried out using 10-cm diameter boreholes combined with pneumatically inflated borehole sealing and measurement assemblies. This assembly consists of an inverted membrane fabricated with mesh pockets to allow the emplacement of filter paper pads and sensors at any desired spacing. The membrane can be inflated to a constant pressure with a pressurization manifold and can be deployed and retrieved periodically using an emplacement canister. The performance of this tracer injection and collection system has been studied using both laboratory experiments (Bussod et al., 1999) and numerical simulations (Tseng and Bussod, 2001). The test activities are subdivided into two main phases each containing different numbers of injection and collection boreholes. The current study is aimed at modeling phase 2 flow and transport.

2.2. Phase 2 layout

The phase 2 test block is a large, 7-m high, 10-m wide, and 10-m deep region with injection and collection in both Calico Hills (Tac) and Topopah Springs (Tptpv1, 2) formations as shown in Fig. 1. A total of eight injection boreholes facing the test alcove were arranged horizontally in two subparallel planes. Three injection rates were designed to balance the need for obtaining timely results with the desire to attain meaningful flow processes for the characterization of the field behavior. Borehole 23, initiated on July 23, 1998, has 10 injection points with a designed injection rate of 1 ml/h. Boreholes 24–27, initiated on July 30, 1998, each has 10 injection points with a designed injection rate of 10 ml/h. Finally, boreholes 18, 20, and 21, initiated on August 5, 1998, each has nine injection points with a designed injection rate of 50 ml/h. All the injection points were separated by a distance of approximately 61 cm. A mixture of multiple conservative, reactive, and colloid-like tracers was injected continuously (i.e., a step input) into the system. The current study focuses on the characterization of conservative tracer (bromide) transport.

Twelve collection boreholes facing the main adit were arranged at various locations perpendicular to the injection boreholes as shown in the figure. Also illustrated in Fig. 1 are the two faults that have been identified in the field and plotted schematically. All the boreholes are horizontal, except boreholes 11 and 47 that are tilted and inclined downwards. Since both field data and preliminary simulations revealed that no solute breakthrough was observed in boreholes 11 and 47, these two boreholes have been removed from further consideration in modeling. The coordinates of each borehole are given in Table 1. Each collection borehole contains a minimum of 15–20 collection pads

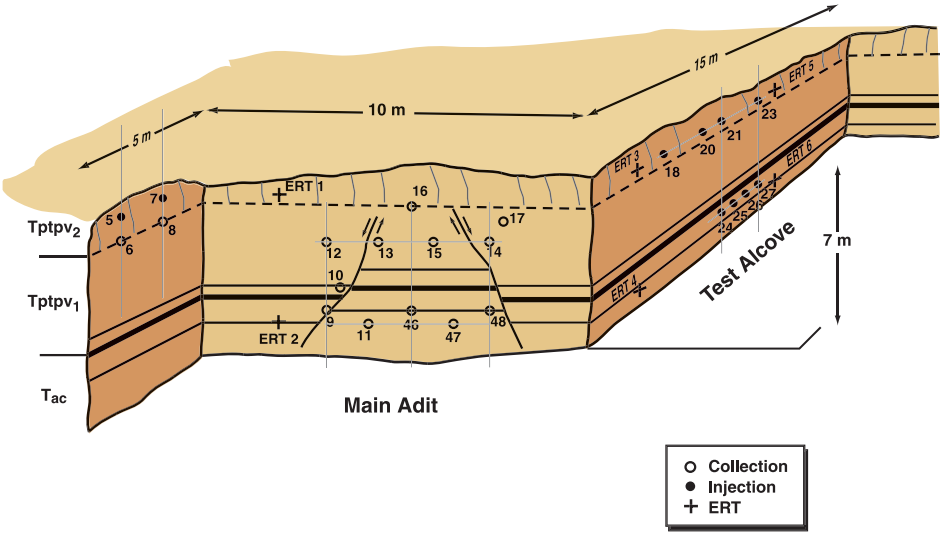

Fig. 1. Schematic of the Busted Butte UZTT phase 2 layout. ERT refers to the electrical-resistance tomography.

distributed along the inverted membrane. Sampling pads are retrieved at regular time intervals (for this case, 7 days) for laboratory analysis of solute concentrations. Based on preliminary laboratory results (Bussod et al., 1999), a 7-day sampling period is needed to establish an equilibrium condition of water potential between the pads and the neighboring porous material. Numerical simulations (Tseng and Bussod, 2001) further demonstrated that, under idealized conditions, the 7-day sampling period used in the field is adequate.

Moisture data were collected using neutron probes at selected times during the membrane retrieving and deploying processes. Neutron probe readings were taken at 10-cm intervals through each borehole. Detailed discussions of the possible influence of a sampling system on the surrounding flow field and the resulting solute transport were given by Tseng and Bussod (2001).

3. Modeling of phase 2 flow and transport

3.1. Conceptual model

It is assumed that the flow and transport of the Busted Butte UZTT can be described using an isothermal, two-phase air–water flow in a rigid porous medium coupled with a convection–dispersion process for the transport of a nonvolatile, nonreactive, dissolved solute. It is further assumed that the physical system of the phase 2 test block is initially under a steady state, equilibrium background flow condition. Simulations of the UZTT were conducted using a finite element heat- and mass-transfer code (FEHM) (Zyvoloski et al., 1997a,b) assuming immiscible, two-

Table 1
Coordinates of boreholes defined at the rock face of each borehole entrance

Borehole number	x (m)[a]	y (m)[b]	z (m)
Injection boreholes			
18	7.17	61.48	− 0.10
20	8.69	61.34	− 0.09
21	9.43	61.46	− 0.11
23	10.92	61.62	− 0.10
24	9.43	61.66	− 4.07
25	9.94	61.81	− 4.07
26	10.43	61.86	− 4.08
27	10.92	62.00	− 4.10
Collection boreholes			
9	3.02	69.38	− 4.26
10	3.18	68.70	− 3.30
11[c]	2.84	68.04	− 4.55
12	3.24	69.30	− 1.40
13	2.87	67.58	− 1.40
14	2.96	64.17	− 1.39
15	2.75	65.88	− 1.40
16	2.84	66.81	− 0.70
17	3.01	63.99	− 0.95
46	2.74	66.74	− 4.25
47[c]	2.58	65.41	− 4.55
48	2.80	64.08	− 4.23

[a] The x-coordinate is defined along the test alcove.
[b] The y-coordinate is defined along the main adit.
[c] Inclined boreholes.

phase flow of pure water and pure air without considering the effects caused by both water vapor and dissolved gas in the system.

The constitutive relationships assumed for this system include first, a non-hysteretic, single-valued functional relationship for both water retention and hydraulic conductivity described by the van Genuchten–Mualem model (van Genuchten, 1980). Second, the dispersion coefficient tensor is proportional to the directional component of the average pore water velocity (Bear, 1972). For this study, a constant value for longitudinal and transverse dispersivity of 5 cm was assumed. Finally, a linear elastic relationship is assumed between phase densities and the corresponding phase pressures. The compressibility of air is thus inversely proportional to its pressure if air is assumed to obey the ideal gas law.

3.2. Simulation approach

3.2.1. Computational grid

Simulations were conducted using a 3-D layered block with two faults imbedded in the computational domain. Based on the field survey, a total of three geologic layers have been incorporated in the system. The local coordinate system extends from 2.5 to 14.5 m in the x-direction (the injection face), from 61 to 74 m in the y-direction

(collection face), and from −8 to 2 m in the vertical *z*-direction. The simulation domain extends at least 2 m away from the edges of the borehole boundaries to avoid any possible boundary effects on simulation results. Preliminary simulations have been performed using various resolutions of numerical grid ranging from a coarse to a more refined one. Results revealed that increasing the resolution from 109,809 to 334,096 nodes does not significantly change the simulation results. Current simulations utilize a variable resolution computational grid with a size decreasing from 0.5 m at and near the domain boundary to approximately 5 cm along the boreholes and the layered interfaces. The entire 3-D domain is comprised of 109,809 unstructured finite element nodes and 626,598 elements.

3.2.2. Hydraulic properties

Laboratory measurements of hydraulic properties were obtained from core samples taken at the boreholes. A total of 51 core samples have been analyzed for retention data whereas for hydraulic conductivity, there are a total of 28 data sets representing all three different hydrologic layers. The representative hydraulic properties for each geologic formation were obtained by fitting the laboratory data to the van Genuchten–Mualem type of model using the RETC code (van Genuchten et al., 1991) as shown in Fig. 2. Different fitting techniques have been exercised. The results revealed that for both Tptpv1 and Tptpv2 layers, almost identical fits can be obtained using different fitting techniques, while for the Tac layer, slight differences can be found when different fitting scenarios were applied. The corresponding parameter sets for the fitted retention and hydraulic conductivity curves are given in Table 2. For the subsequent flow and transport simulations, the parameter sets obtained from the simultaneous fit of retention and hydraulic conductivity data were used. The hydraulic properties were assumed to be homogeneous within each layer.

3.2.3. Injection rates

The true injection rate for each borehole appears to fluctuate considerably with its mean rate being in general less than the designed rate as shown in Table 3. A test run has been conducted to compare the simulation results using both the true injection rates and their corresponding mean rates. It appears that both simulations yielded almost identical results. In the subsequent simulations, a constant mean injection rate for each borehole was assumed for the purpose of saving computational time.

3.2.4. Initial and boundary conditions

The procedures used in this study were to first generate a steady state, equilibrium background flow field using appropriate boundary conditions. This steady flow field then serves as the initial condition for the flow and transport simulations. One way to define an appropriate boundary condition is to use the neutron moisture data measured at the uppermost Tptpv2 layer boreholes (i.e., boreholes 18, 20, 21, and 23) before the experiments are initiated. The moisture data, measured every 10 cm along each collection borehole, show a variation between 12% and 15% with mean volumetric water content of approximately 13.5%. It is assumed that the upper boundary of the

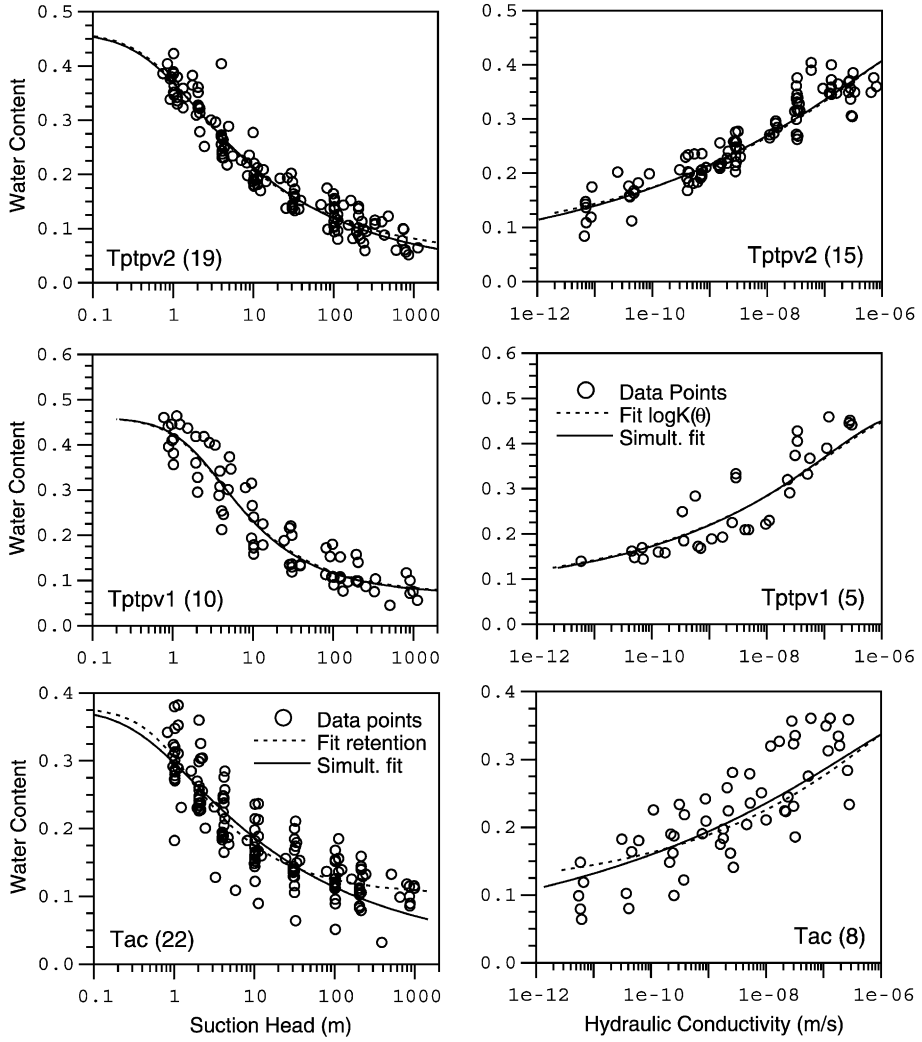

Fig. 2. Fitting of retention and hydraulic conductivity curves. The numbers in the parentheses indicate the number of core samples included in the analysis.

system has constant ambient water saturation equivalent to 13.5% of volumetric water content. The lateral boundaries were assumed to be a no-flux-type condition. The lower boundary was taken as gravity-drained boundary condition. For airflow, both upper and lower boundaries were assumed to be at a constant air pressure of 0.101 MPa, whereas the lateral boundaries were taken as a no-flux condition.

A simulation was conducted by applying these boundary conditions for a period of time sufficient for the system to reach equilibrium. A flow and transport simulation was then initiated while maintaining these boundary conditions as the background flow field. The

Table 2
Hydraulic parameter sets obtained from different optimization techniques

	Saturated hydraulic conductivity, K_{sat} (m/s)	Residual water content, θ_r	Saturated water content, θ_s	α (1/m)	n
Fit retention data					
Tptpv2	–	0.049	0.463	1.432	1.351
Tptpv1	–	0.068	0.461	0.511	1.517
Tac	–	0.102	0.379	1.308	1.515
Fit log of conductivity data[a]					
Tptpv2	0.268×10^{-4}	–	–	–	–
Tptpv1	0.346×10^{-5}	–	–	–	–
Tac	0.139×10^{-4}	–	–	–	–
Simultaneous fit[b]					
Tptpv2	0.359×10^{-4}	0.023	–	1.595	1.300
Tptpv1	0.286×10^{-5}	0.068	–	0.479	1.541
Tac	0.573×10^{-4}	0.013	–	2.253	1.238

[a] Fit log $K(\theta)$ for K_{sat} only, other parameters were taken from retention fit.
[b] Assume porosity (i.e., θ_s) values were known (taken from retention fit).

solute injection was taken as a flux-type condition along with water injection at the injection points.

4. Results

Both observed and simulated results can be separated into three groups of similar characteristics. The first group is the upper portion of the upper collection that contains boreholes 16 and 17. The second group pertains to the lower portion of the upper collection with boreholes 12, 13, 14, and 15. Finally, the third group contains all the lower collection boreholes (9, 10, 46, and 48) with borehole 10 as an exception characterized in terms of its observed flow and transport. Comparisons of the observed and simulated flow and transport results are given in the next two sections. Further discussions on the

Table 3
Statistics of the borehole injection rates

Borehole number	Designed injection rate (ml/h)	True injection rate, I (ml/h)			
		Mean	Variance	I_{max}	I_{min}
18	50	37.97	53.51	54.30	0.00
20	50	38.40	39.71	47.10	0.00
21	50	36.14	54.74	44.80	0.00
23	1	0.81	0.05	3.79	0.05
24	10	8.16	2.63	11.40	0.00
25	10	6.89	3.60	11.00	0.00
26	10	7.46	2.01	10.30	0.00
27	10	7.71	2.27	10.50	0.00

deficiencies in using the current model to describe the flow and transport processes at the field are summarized in Section 4.3.

4.1. Flow field

Figs. 3 and 4 show a comparison of observed and simulated water content profiles along the collection boreholes at selected times. Also shown in the figures are the relative locations of the injection boreholes for easy reference. In general, field observations revealed that the system reached a quasi-steady state flow condition beneath the injection boreholes several months after the commencement of injection while leaving some lateral spreading that can be observed on the moisture profiles. The simulation results, on the other hand, showed a strong transient flow field, and the predicted water contents were generally higher than those measured in the field.

The apparent steady state condition in field observations can be an artifact due to the measurement itself. The neutron measurements represent a volume average of approximately 50 cm in diameter depending on both the formation property and the moisture content. The estimated measurement uncertainty for volumetric water content is in the range from $\pm 0.14\%$ to $\pm 0.24\%$. In the relatively dry range of the retention values, the uncertainty of the measured data may have overwhelmed the slight change of moisture that actually occurred in the system. However, the corresponding changes in matrix potential pressure head can be so significant that the system is still driven by capillary force.

Similar artifact is also expected for the strong transient conditions revealed in simulation results. It is generally accepted that the system dynamics within the dry range is not fully understood and the retention property not well defined. van Genuchten et al. (1991) have cautioned the use and interpretation of retention curves near the dry range. The hydraulic properties used in the conceptual model (Fig. 2 and Table 2) may have been biased to the predicted system behavior and hence resulted in noticeable differences as compared to field observations.

Note that all the upper collection boreholes (12–17) have been identified in our current study to be in the same hydrologic layer of Tptpv1, hence they share the same hydraulic properties in the simulation. As such, the simulation showed similar results for all these boreholes. However, field observations indicate that the upper portion (boreholes 16 and 17) and the lower portion (boreholes 12–15) might display different behaviors due to the generally lower water content observed in boreholes 12–15. Also note that boreholes 12–15 revealed a high initial water content in the deep end of the boreholes, which does not occur in boreholes 16 and 17. This may be caused by a material property difference within or between the upper and lower portions that is not identified in our current study.

For the lower collection boreholes within the Tac layer, similar results were found among boreholes 9, 46, and 48. Borehole 10 is located above injection boreholes 24–27. The results of borehole 10 revealed a gradual increase in water content, indicating that the system is largely a capillary-dominated flow condition under the applied injection rates. An analysis by Tseng and Bussod (2001) using Philip's definition (a dimensionless parameter γ expressed as a function of sorptive number and the characteristic length scale, see Philip et al., 1989) showed that water flow in the Calico Hills tuff is primarily dominated by capillarity even under a relatively wet range. For Tptpv2 layer, the

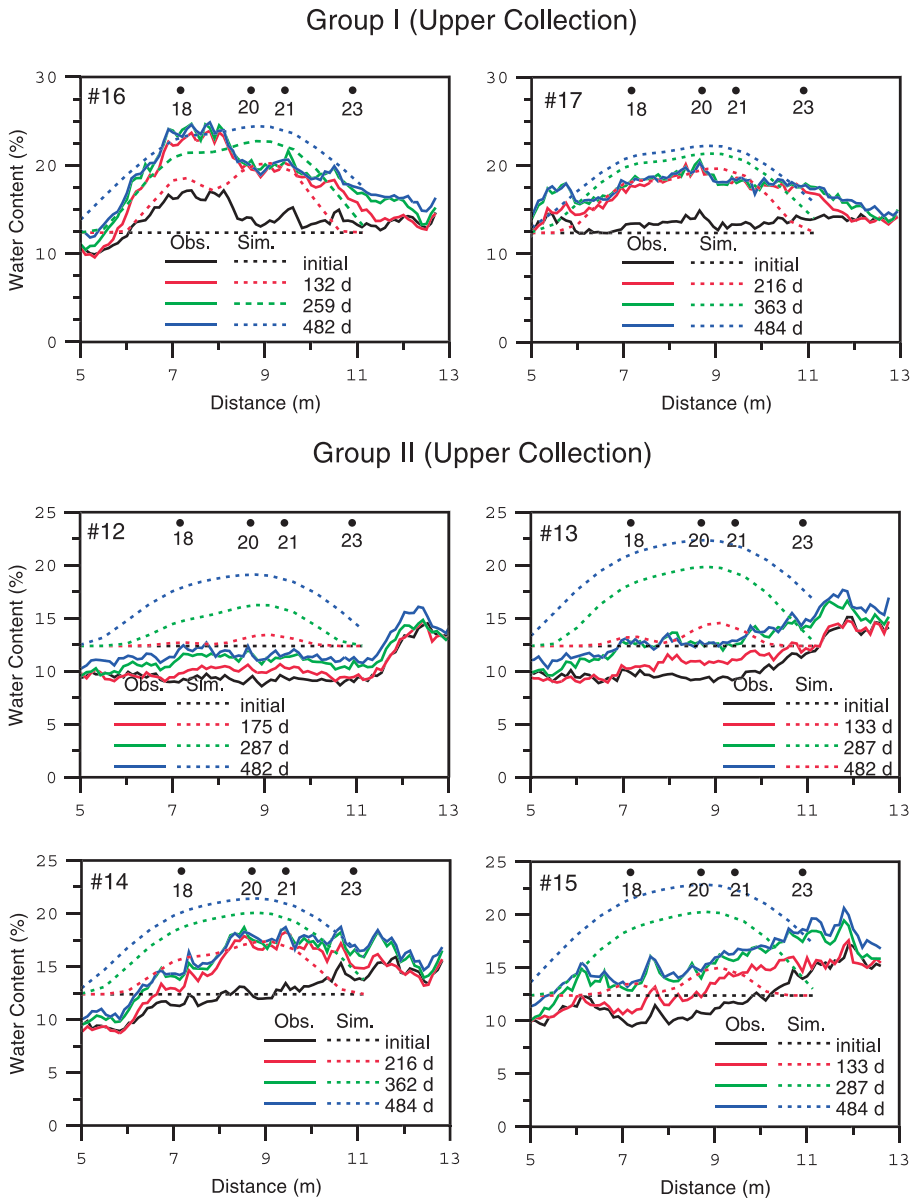

Fig. 3. Comparison of simulated and field-measured neutron moisture profiles in the upper collection boreholes at selected times.

simulation results (not shown) revealed that under the 50 ml/h injection rate, the flow field is also capillary dominated. The propagation of water started as a spherical pattern growing from a point injection and eventually became more cylinder-like, growing around

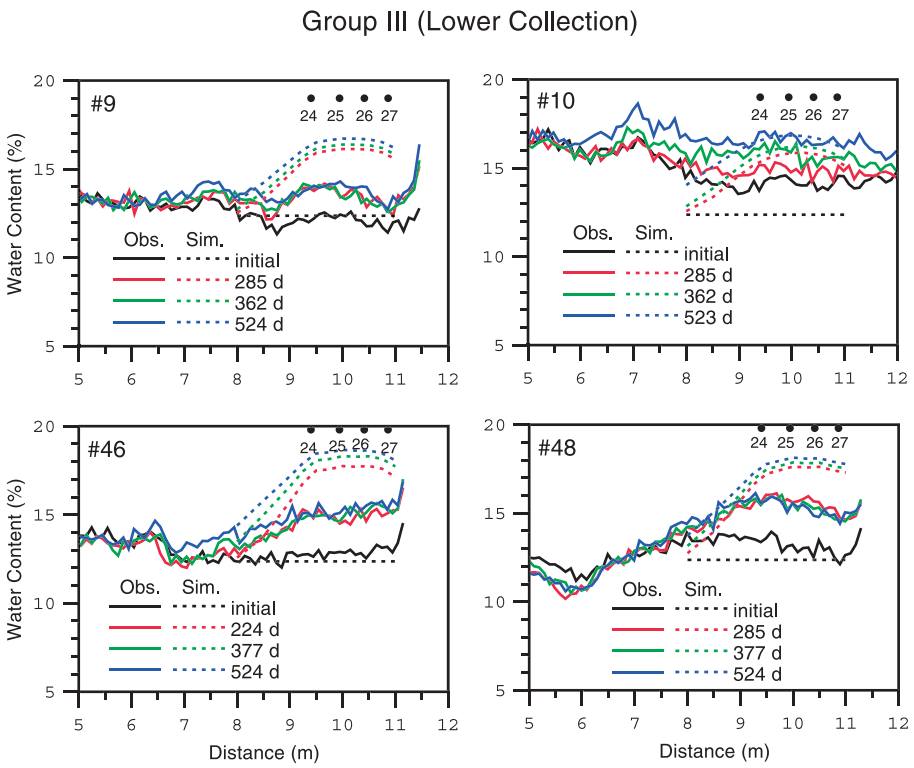

Fig. 4. Comparison of simulated and field-measured neutron moisture profiles in the lower collection boreholes at selected times.

each injection borehole as its center. Further evidence of strong, capillary-driven flow and transport was obtained during the mineback and overcoring of the phase 1 experiments (Bussod et al., 1999).

4.2. Solute transport

Fig. 5 shows a comparison of observed and simulated solute resident concentrations taken along the collection boreholes at selected times. One representative borehole has been selected for each of the three groups that show similar characteristics. Also shown in the figure is the result of borehole 10 that behaves differently from the three groups defined.

The upper portion of the upper collection boreholes (16 and 17) generally shows a better match. However, the observed solute concentration distributions decreased at 239 days as compared to those at 183 days, and no increase in peak concentration was observed at 337 days for borehole 16. Since solute injection was a step function, this decrease in concentration was not captured in the simulation. The simulated solute concentration profiles, hence, depicted an early underestimation to a later overestimation for both boreholes 16 and 17. This is partly due to the concentration drops observed in the

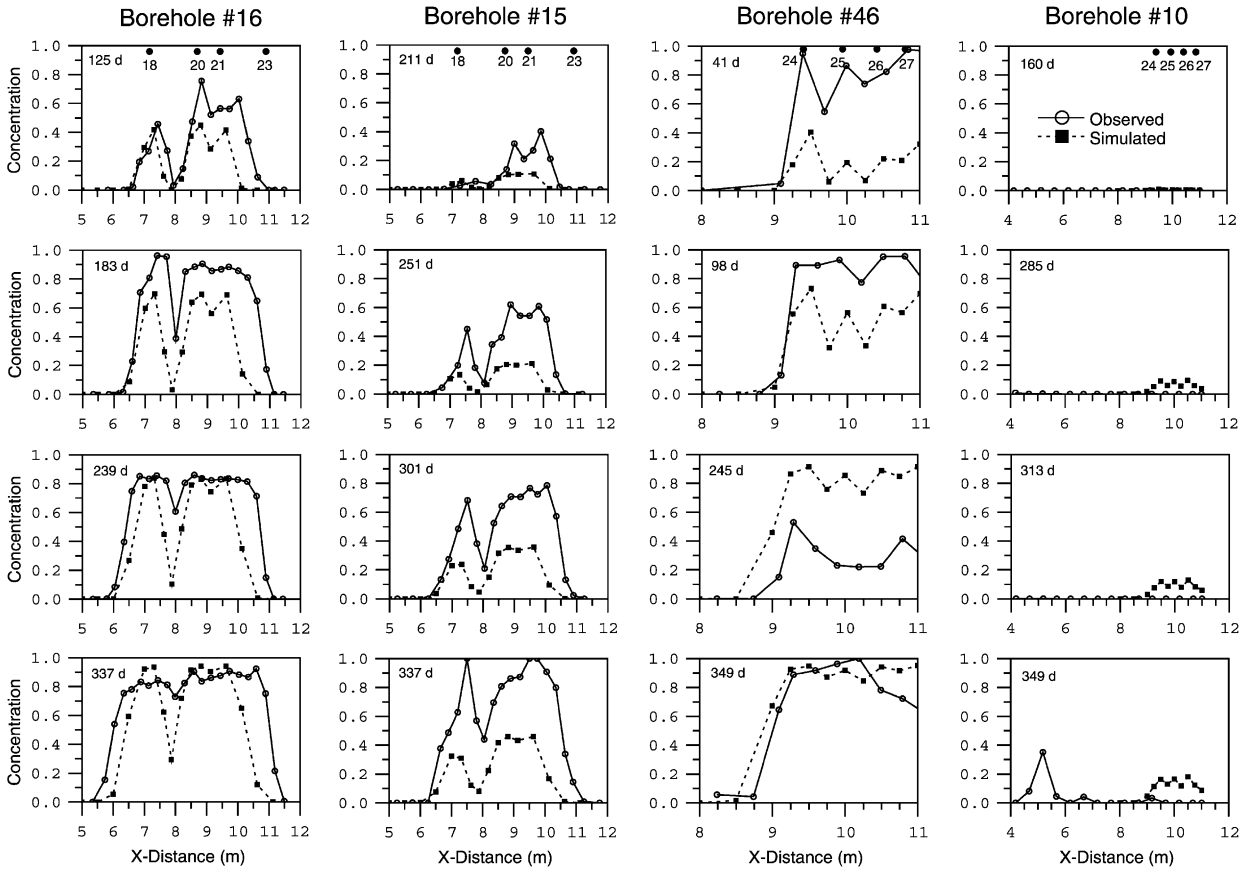

Fig. 5. Comparison of observed and simulated solute concentration profiles at selected times on four representative boreholes.

field at times. The difference in the flow field of a quasi-steady state versus transient also contributed partly to the explanation of this inconsistency in estimation. The lower portion of the upper collection (boreholes 12–15) shows a consistent underestimation in concentration although some very slight, noise-like decrease of measured concentration is still present at times for those boreholes.

The lower layer includes boreholes 9, 10, 46, and 48. Boreholes 9, 46, and 48 all have a more dramatic concentration drop, with borehole 46 having the most significant one as shown in the figure. Fig. 6 further illustrates the concentration drop of borehole 46 when plotted as a function of time at selected locations. We can observe an instant breakthrough of solute at $x = 9.09$ m accompanied with a dramatic decrease to near detection limit followed by gradual increase and decrease as time elapses. It appears that the decreases in concentration occurred at the same time in different locations along borehole 46. However, the same is not always true for all the boreholes. Each borehole displays different patterns of increase and decrease in observed concentrations, and those significant decreases occur at different times for different boreholes.

Note that for borehole 9 (not shown), the field observation showed only one concentration peak corresponding to the injection of borehole 24. The breakthrough of solute from other injection boreholes (i.e., 25, 26, and 27) was detected at a much later time. Borehole 10, which is located above the injection boreholes 24–27, did not break through at early times as predicted. Instead, breakthrough was detected after 349 days at an unexpected location away from the injection boreholes as depicted in Fig. 5.

4.3. Summary and discussion

There are a number of possibilities that can cause a decrease in measured concentrations even though solute was continuously injected. For instance, imperfect contact of

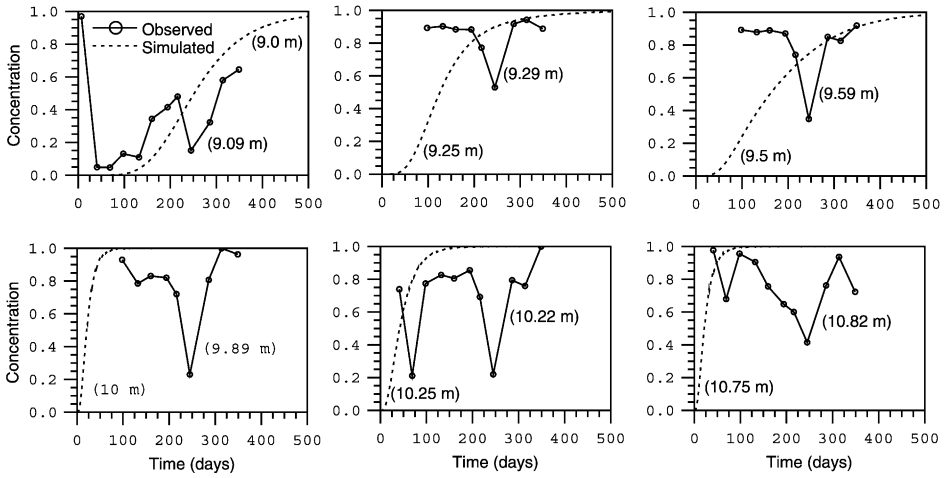

Fig. 6. Comparison of observed and simulated solute breakthrough curves at selected locations within borehole 46.

the collection pads to the borehole wall due to operational problems. If this is the case, a sudden drop followed by an increase back to the normal value during consecutive measurements is to be expected. The field measurements revealed that both a sudden and a gradual drop of concentrations have occurred during the observations. Moreover, a more gradual increase of several measurements for the concentrations to reach the previous level has also been observed, implying that some physical process may be responsible for this phenomenon.

One possible cause of the concentration fluctuations not included in our model could be due to the inherent heterogeneity of the tuff formation, including the possible fracture and matrix interactions. Tseng and Jury (1994) showed that a wealth of structure in the measured concentration profiles could be observed using numerical experiments in a hypothetical, Miller-similar medium. Roth (1995) and Roth and Hammel (1996) further demonstrated that concentration redistribution could occur during the transition of the hydraulic structure from one state to another at different saturation conditions. The possible fracture/matrix flow and transport suggest another mechanism that may contribute to the observed concentration fluctuations and hence complicate the analysis of the physical system.

Further complication could be due to an unintended drying during field operation. In semiarid regions, potentially significant evaporation plays an important role that may dry the boreholes and the sampling pads fairly quick. In effect, it produces an artifact of higher concentration to various degrees. This drying process may be responsible for the unexpected instant breakthrough as illustrated on the upper left corner of Fig. 6. It may also be responsible for the explanation of concentration decreases. The seemingly impossible cause due to imperfect contact, as described above, may actually be true when drying overwhelms the internal physical processes during consecutive measurements. The combined effect of drying and imperfect contact of sampling pads explains in part the observed concentration fluctuations.

Based on the field survey of the faults' locations using linear interpolation, different scenarios have been implemented by including faults as either an extremely conductive material (a discrete fracture) or as a barrier. Since a fault crosses a borehole at only one particular location, including faults in the simulations does not improve the general match of a solute profile in the simulation results as compared to the field observations. The two faults cross borehole 9 at $x = 3.65$ and 7.85 m, respectively. The presence of faults does not explain the observed single solute peak corresponding to the injection of borehole 24 and the much delayed solute breakthrough from boreholes 25–27, as described in the previous section. For borehole 10, the two faults cross it at $x = 3.73$ and 7.30 m, respectively. Simulation revealed that no solute breakthrough was detected at these two locations when assuming fault as a discrete fracture. On the other hand, field observation showed an unexpected solute breakthrough at $x = 5$ m in borehole 10, suggesting that more detailed field survey is needed for a better explanation of this discrepancy.

Sensitivity studies show that the van Genuchten parameter n is the most sensitive parameter for the Tac layer under the designed injection rate of 10 ml/h. For the Tptpv1 layer, both the parameters α and n are equally sensitive. Although it is generally recognized that the effective porosity can be much smaller than the laboratory measured porosity, adjusting the porosity values may improve the estimation of some boreholes

(e.g., boreholes 12–15) but deteriorate that of others (i.e., boreholes 16 and 17). Similarly, an improvement in the predictions at the early times will result in deterioration at a later time, or vice versa, for a number of boreholes. Increasing the dispersivity values results in an earlier breakthrough and a lower peak concentration accompanied by a wider spreading at a given time. Although the dispersivities and their transition from an early time local value to an asymptotic dispersivity may play a role in explaining the field observations, it is believed that the hydraulic properties are of more importance in controlling the transport processes of this system.

5. Concluding remarks

The current model is able to capture some qualitative features and general characteristics of the system with variable success. Both numerical simulations and field observations revealed a capillary-dominated flow field within this system. The representation of the estimated model parameters may eventually become important factors for unsaturated flow and transport simulations. Issues identified in this study will serve as a guide to a refined modeling study. Material properties of the Tptpv1 layer need to be investigated in more detail for a proper explanation of the differences observed in its upper portion (boreholes 16 and 17) and the lower portion (boreholes 12–15). Other approaches such as the Warrick scaling (Warrick et al., 1977) and the inverse modeling techniques may prove to be a valuable tool in looking into the relationships between hydraulic properties and the resulting flow and transport processes. Finally, the possible causes of the observed concentration drops need to be identified for a better understanding of this physical system.

Acknowledgements

This research was supported by the Yucca Mountain Site Characterization Program Office as part of the Civilian Radioactive Waste Management Program. This project is managed by the US Department of Energy, Yucca Mountain Site Characterization Project. The retention and hydraulic property data were obtained from Lorraine Flint of USGS. The injection rates and the neutron moisture data were obtained from the Science and Engineering Associates (SEA). The authors thank John H. Kessler, Hari Viswanathan, and an anonymous reviewer for their thorough review of this manuscript.

References

Bear, J., 1972. Dynamics of Fluids in Porous Media. Elsevier, New York.

Bussod, G.Y., Turin, H.J., Lowry, W.E., 1999. Busted Butte unsaturated zone transport test. Report LA-13670-SR. Los Alamos National Laboratory.

Eisenberg, N.A., Lee, M.P., Federline, M.V., Wingefors, S., Andersson, J., Norrby, S., Sagar, B., Wittmeyer, G.W., 1999. Regulatory perspectives on model validation in high-level radioactive waste management programs: a joint NRC/SKI white paper. Report NUREG-1636. US Nuclear Regulatory Commission.

Philip, J.R., Knight, J.H., Waechter, R.T., 1989. Unsaturated seepage and subterranean holes: conspectus, and exclusion problem for circular cylindrical cavities. Water Resour. Res. 25, 16–28.

Roth, K., 1995. Steady state flow in an unsaturated, two-dimensional, macroscopically homogeneous, Miller-similar medium. Water Resour. Res. 31 (9), 2127–2140.

Roth, K., Hammel, K., 1996. Transport of conservative chemical through an unsaturated two-dimensional Miller-similar medium with steady state flow. Water Resour. Res. 32 (6), 1653–1663.

Tseng, P.-H., Bussod, G.Y., 2001. Evaluation of the filter paper technique for in situ sampling of solute transport in unsaturated soils and tuffs. Water Resour. Res. 37 (7), 1913–1928.

Tseng, P.-H., Jury, W.A., 1994. Comparison of transfer function and deterministic modeling of area-averaged solute transport in a heterogeneous field. Water Resour. Res. 30 (7), 2051–2063.

van Genuchten, M.T., 1980. A closed-form equation for predicting the hydraulic conductivity of unsaturated soils. Soil Sci. Soc. Am. J. 44, 892–898.

van Genuchten, M.T., Leij, F.T., Yates, S.R., 1991. The RETC code for quantifying the hydraulic functions of unsaturated soils. Report EPA/600/2-91/065. US Environmental Protection Agency.

Warrick, A.W., Mullen, G.J., Nielsen, D.R., 1977. Scaling field-measured soil hydraulic properties using a similar media concept. Water Resour. Res. 13, 355–362.

Zyvoloski, G.A., Robinson, B.A., Dash, Z.V., Trease, L.L., 1997a. Summary of the models and methods for the FEHM application—a finite element mass- and heat-transfer code. Report LA-13307-MS. Los Alamos National Laboratory.

Zyvoloski, G.A., Robinson, B.A., Dash, Z.V., Trease, L.L., 1997b. User's manual for the FEHM application—a finite element mass- and heat-transfer code. Report LA-13306-M. Los Alamos National Laboratory.